Electronic Supplementary Information (ESI)

Coordination-Modulated Piezochromism in Metal-Viologen Materials

Qi Sui, *Ye Yuan*, *Ning-Ning Yang*, *Xin Li*, *Teng Gong*, *En-qing Gao*,[*] *and Lin Wang*[*]

Physical measurements

The FT-IR spectra were recorded in the range 500-4000 cm^{-1} using KBr pellets on a Nicolet NEXUS 670 spectrophotometer. Elemental analyses were performed on an Elementar Vario ELIII analyzer. Thermogravimetric analyses (TGA) were carried out on a Mettler Toledo TGA/SDTA851 instrument under flowing air at a heating rate of 10℃/min. Powder X-ray diffraction (PXRD) at ambient pressure was recorded on a Rigaku D/Max-2500 diffractometer at 35 kV, 25 mA for a Cu-target tube and a graphite monochromator. Optical diffuse reflectance (UV-vis) spectra were measured using a SHIMADZU UV-2700 spectrophotometer, with $BaSO_4$ plates as references (100% reflection). Electron spin resonance (EPR) spectra were recorded on a Bruker Elexsys 580 spectrometer with a 100 kHz magnetic field in the X band at room temperature. X-ray photoelectron spectroscopy (XPS) studies were performed with a PHI 5000 Versaprobe spectrometer using Al Kα radiation ($\lambda = 8.357$ Å). To compensate for surface charging effects, all XPS spectra were referenced to the C 1s neutral carbon peak at 284.6 eV. The *in-situ* UV-vis absorption measurements under high pressure are performed on an Ocean Optics QE65000 scientific-grade spectrometer with a DAC (500 µm culets) containing a single crystal of 1. A ruby sphere was loaded to determine pressure by using the ruby fluorescence,[1] and silicone oil was used as a pressure-transmitting medium. The high pressure experiment was conducted at room temperature.

Computations

Based on the X-ray crystallographic data of 1, DFT (density functional theory) calculations were performed to analyze the density of states (DOS) and the frontier orbitals. The DMol^3 module[2] in the Materials Studio software package[3] was used with fine accuracy for the numerical integration of the Hamiltonian and a fine (10^{-6} eV/atom) tolerance for SCF convergence. The DFT exchange-correlation potential was described by the Perdew−Burke−Eruzerhof (PBE) functional within the generalized gradient approximation (GGA).[4] The Tkatchenko-Scheffler (TS) scheme was applied for dispersion corrections.[5] All electrons were included in the calculations and the DNP (double numerical plus polarization) basis set was used with a fine orbital cutoff quality. Geometry optimization of the crystal structure in the absence and presence of external pressure

was performed using the CASTEP program.[6] The optimization applied the GGA-PBE exchange-correlation functional and the TS dispersion-correction scheme. The optimization convergence was judged by an energy tolerance of 10^{-5} eV/atom, a maximum displacement of 0.001 Å, and a maximum force threshold of 0.03 eV/Å. The norm-conserving pseudopotentials in reciprocal space were used for the electronic Hamiltonian, with a SCF convergence tolerance of 10^{-6} eV/atom.

References:

1. H. K. Mao, J. Xu and P. M. Bell, *J. Geophys. Res., B*, 1986, 91, 4673-4676.

2. (a) B. Delley, *J. Chem. Phys.*, 2000, 113, 7756-7764; (b) B. Delley, *J. Chem. Phys.*, 1990, 92, 508-517.

3. *Materials Studio. version 5.0.0. Accelrys Software Inc.: San Diego, CA*, 2009.

4. J. P. Perdew, K. Burke and M. Ernzerhof, *Phys. Rev. Lett.*, 1996, 77, 3865-3868.

5. A. Tkatchenko and M. Scheffler, *Phys. Rev. Lett.*, 2009, 102, 3005.

6. S. J. Clark, M. D. Segall, C. J. Pickard, P. J. Hasnip, M. J. Probert, K. Refson and M. C. Payne, *Z. Kristallogr.*, 2005, 220, 567-569.

Supplementary Tables

Table S1 The hydrogen bonds of compound **1**.

D-H	d (D-H)	d (H···A)	< DHA	d (D···A)	A
C6-H6A	0.950	2.578	130.76	3.278	O6 [x+1/2,-y+2,z]
C8-H8A	0.950	2.464	126.78	3.127	O3 [x-1/2,-y,z]
C12-H12A	0.950	2.380	131.77	3.095	O4 [-x+1/2,y+1,z+1/2]
C16-H16A	0.950	2.377	146.54	3.212	O2 [-x+1/2,y-1,z-1/2]
C17-H17A	0.950	2.456	153.04	3.330	O4 [x,y+1,z]
C23-H23A	0.950	2.592	128.6	3.270	O8 [-x,-y+1,z-1/2]

Table S2 The experimental and optimized lattice parameters and geometrical parameters of compound **1**.
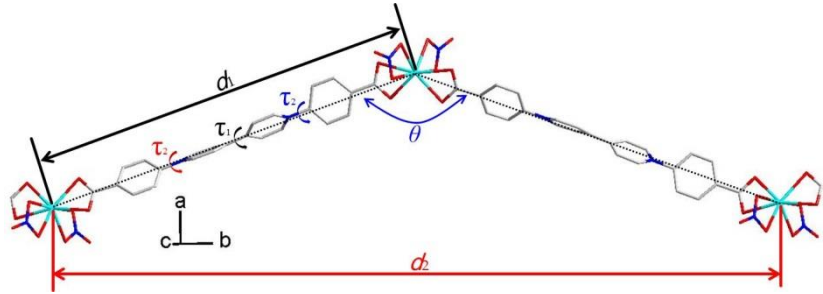
	Exp. Data	at 0 GPa	at 3.5 GPa
V / Å^3	2461.04(12)	2487.4	2067.0
a	15.6931(4)	15.57	14.55
b	10.3418(3)	10.32	10.48
c	15.1640(4)	15.48	13.55
d_1 / Å	23.6883(9)	23.66	23.42
d_2 / Å	44.0590(13)	44.09	44.05
θ / °	136.861(2)	137.39	140.24
τ_1 / °	28.51(28)	28.71	29.14
τ_2 / °	46.91(27)	42.39	40.05
τ_3 / °	66.94(31)	64.85	59.11
cross angle [a] / °	40.26	41.10	35.84
O2$\cdots$H16 / Å	2.3773(60)	2.40	1.96
O9$\cdots$H16 / Å	2.4245(95)	2.24	2.25
O4 $\cdots$H12 / Å	2.3803(60)	2.25	2.16
Interchain distance [b] / Å	3.56	3.62	3.22
Interlayer distance [c] / Å	7.84	7.78	7.28

[a] The acute angle between the two different propagation directions of chains. [b] The distance between neighboring parallel chains in a layer. [c] The distance between neighboring layers.

Table S3 The lattice parameters and donor-acceptor distances of the 3D MOF **2.**

	Exp. Data	Optimization at 3.5 GPa
V / $\mathring{A}^3$	4337.5(28)	4119.77
a	18.196(5)	18.11
b	18.196(5)	18.11
c	15.127(5)	14.50
$N \cdots Cl$ / $\mathring{A}$	3.408(8)	3.39
$N \cdots O$ / $\mathring{A}$	3.579(8)	3.32

Supplementary Figures
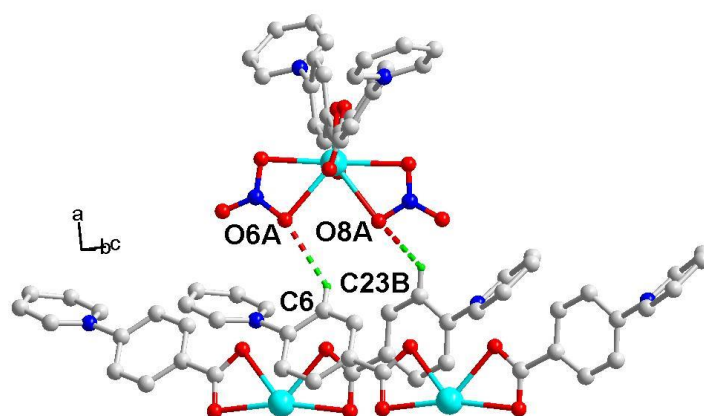
Fig. S1. Hydrogen bonds between chains from different layers in compound **1**. Symmetry code: A

= 0.5+x, 2-y, z; B = 0.5-x, 1+y, 0.5+z;
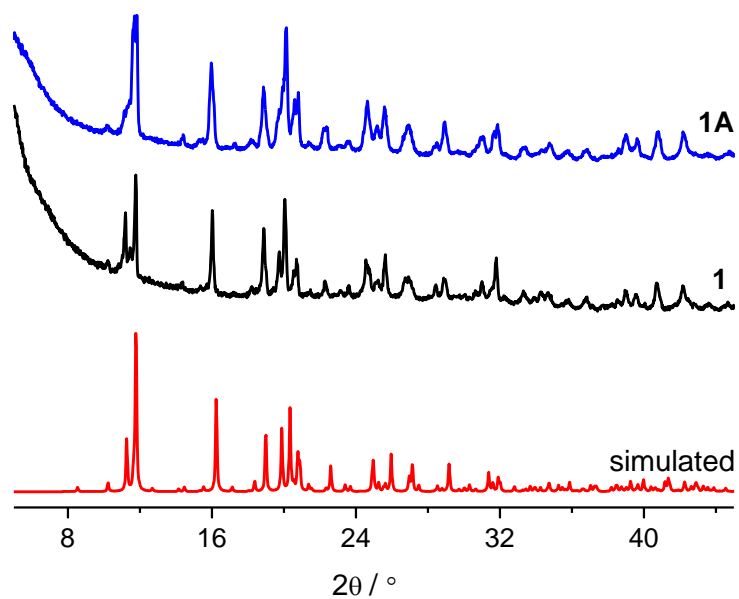
Fig. S2. The PXRD profiles of compound **1** (before compression) and **1A** (after compression).
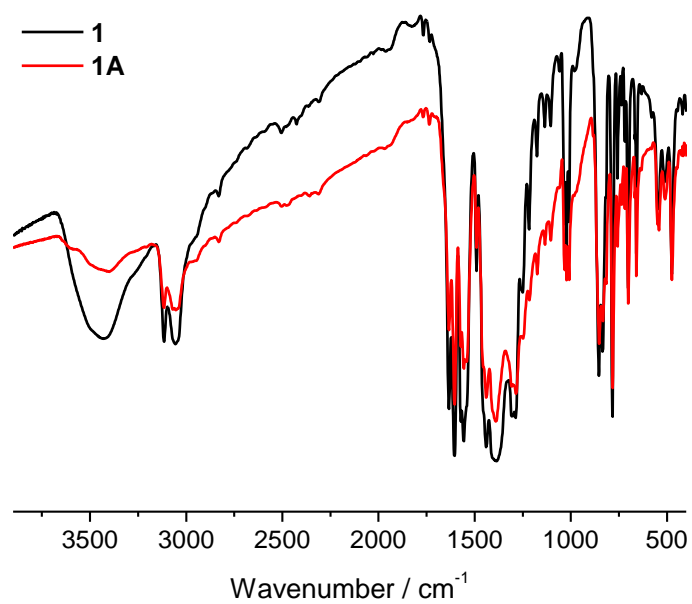
Fig. S3. The IR spectra of **1** (before compression) and **1A** (after compression).
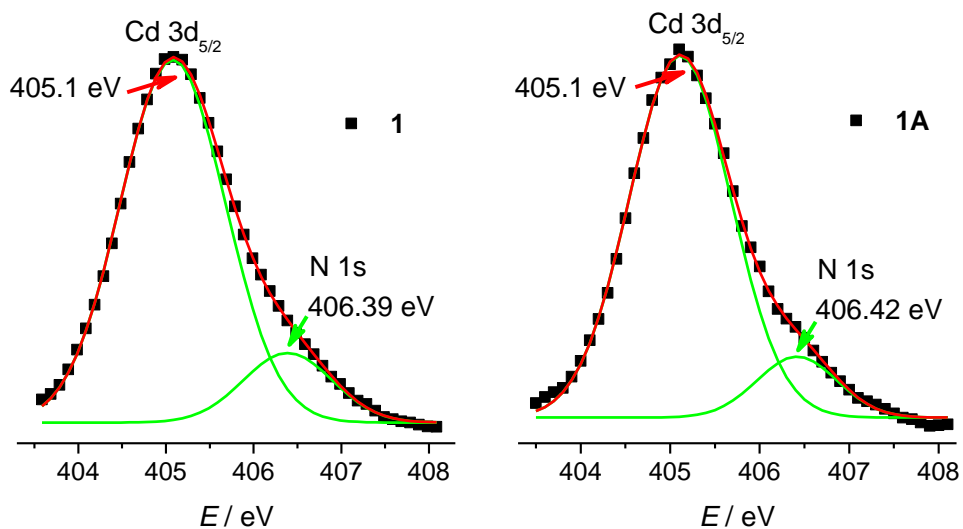
Fig. S4. The XPS spectra of Cd $3d_{5/2}$ and N 1s in compound **1** (before compress) and **1A** (after compress) and the multi-peak resolution.
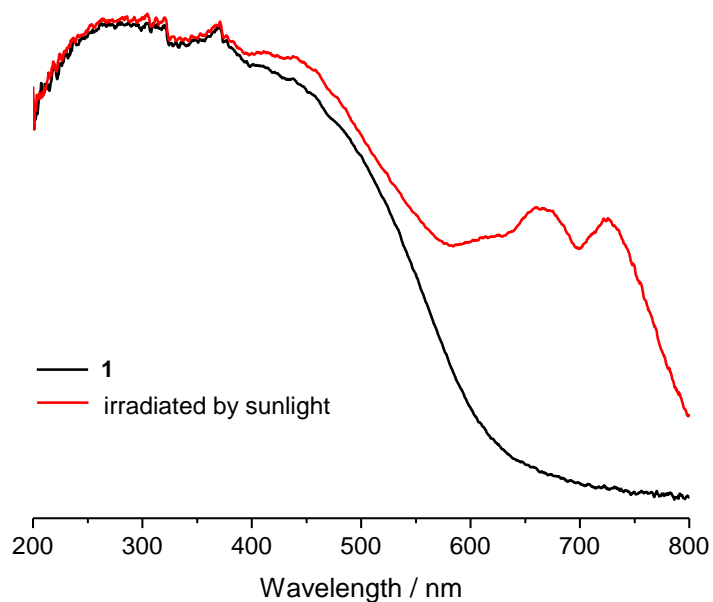

Fig. S5. UV-vis spectra of the compound **1** before and after irradiation under sunlight for 15 mins.
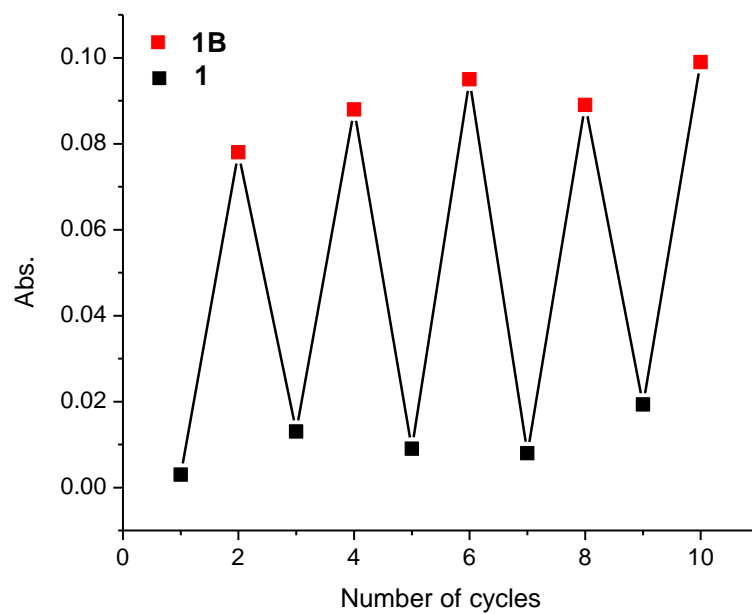
Fig. S6. The repeated cycles of **1** (before irradiation) and **1B** (after irradiation with Xe lamp) (based on absorbance at $\lambda = 726$ nm).
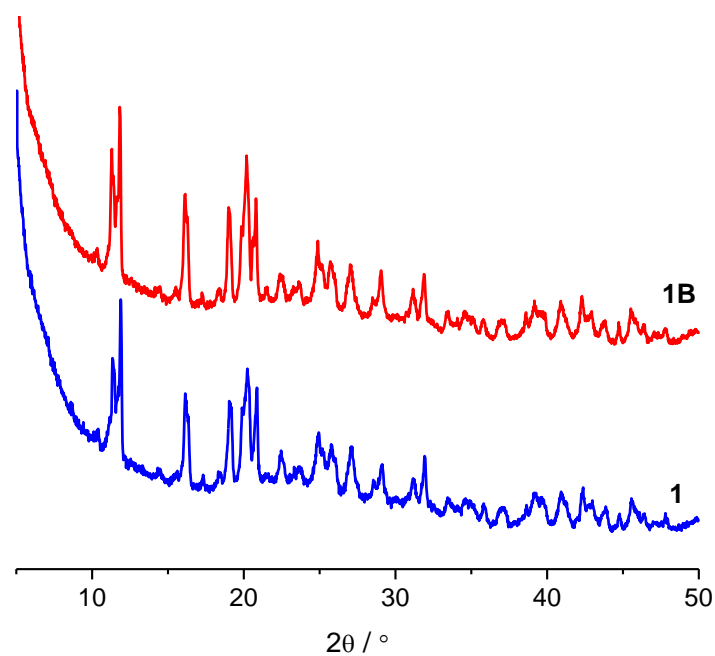

Fig. S7. The PXRD profiles of **1** (before irradiation) and **1B** (after irradiation with Xe lamp).
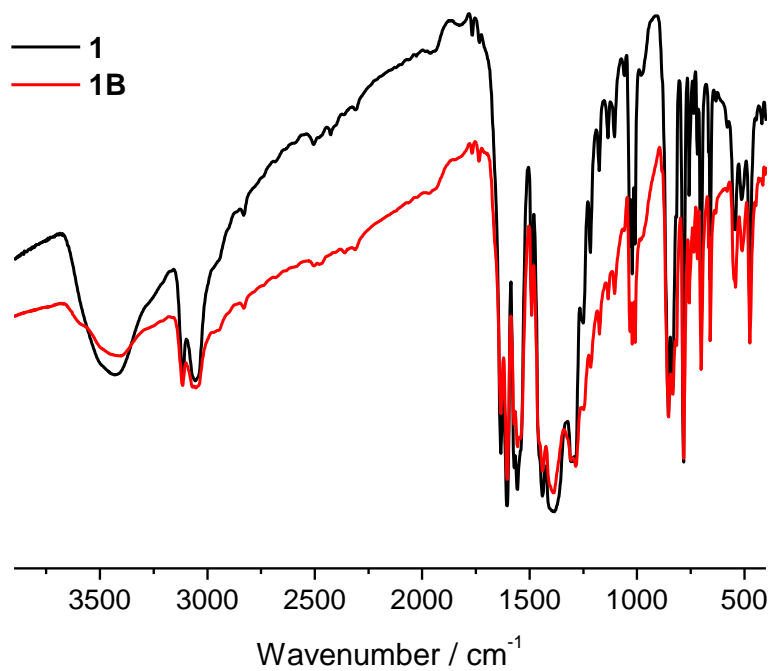
Fig. S8. The IR spectra of **1** (before irradiation) and **1B** (after irradiation with Xe lamp).
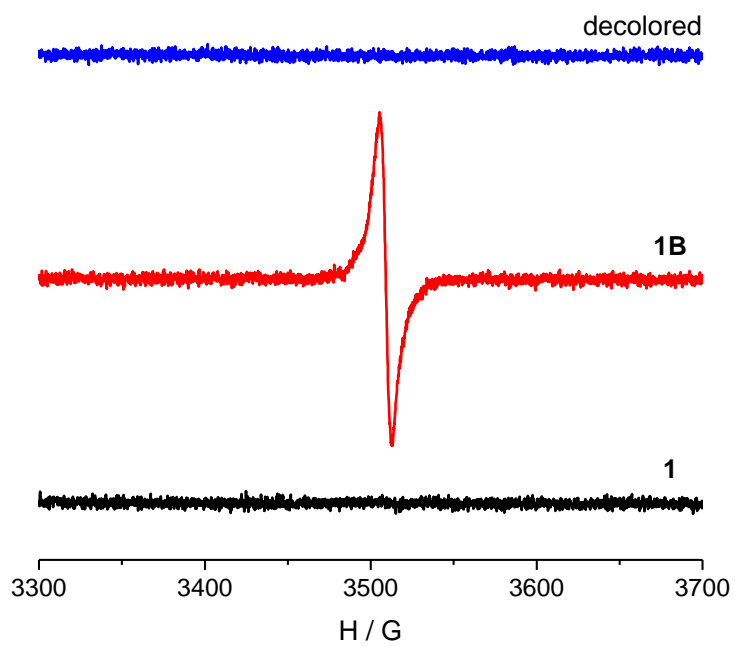

Fig. S9. The EPR spectra of **1** (before irradiation) and **1B** (after irradiation with Xe lamp).
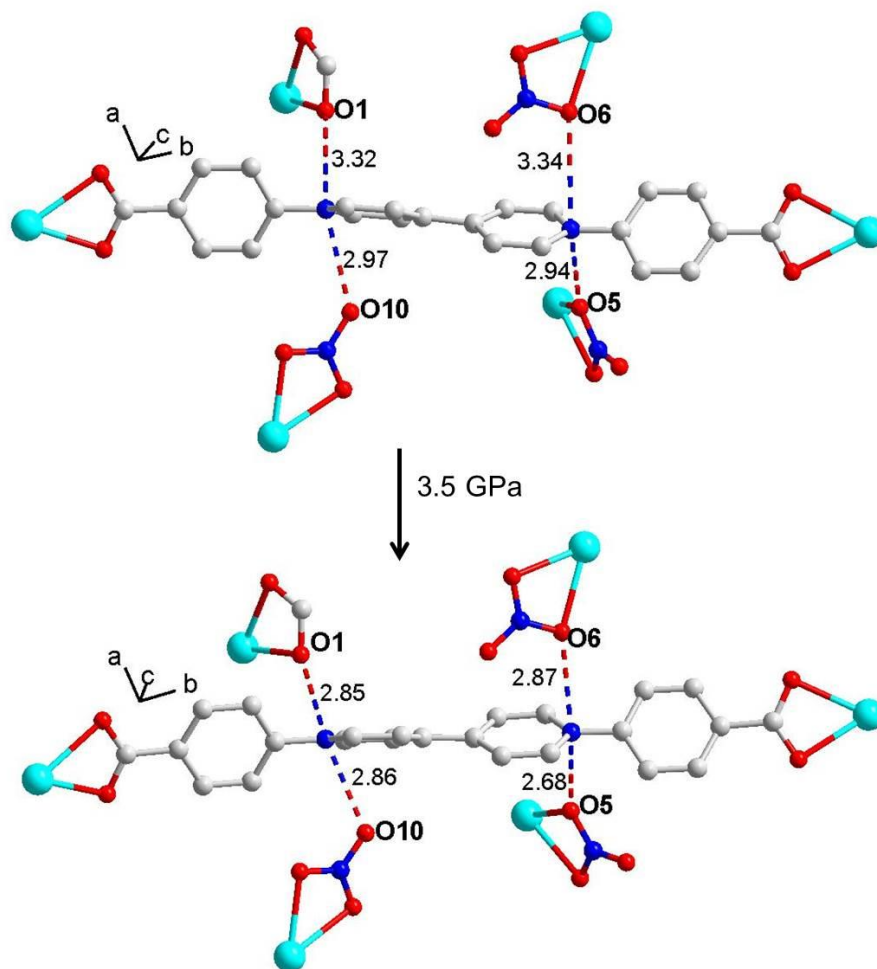
Fig. S10 Pressure-induced changes of donor-acceptor contacts in compound **2** (the structure was drawn according to the results of DFT geometry optimization).
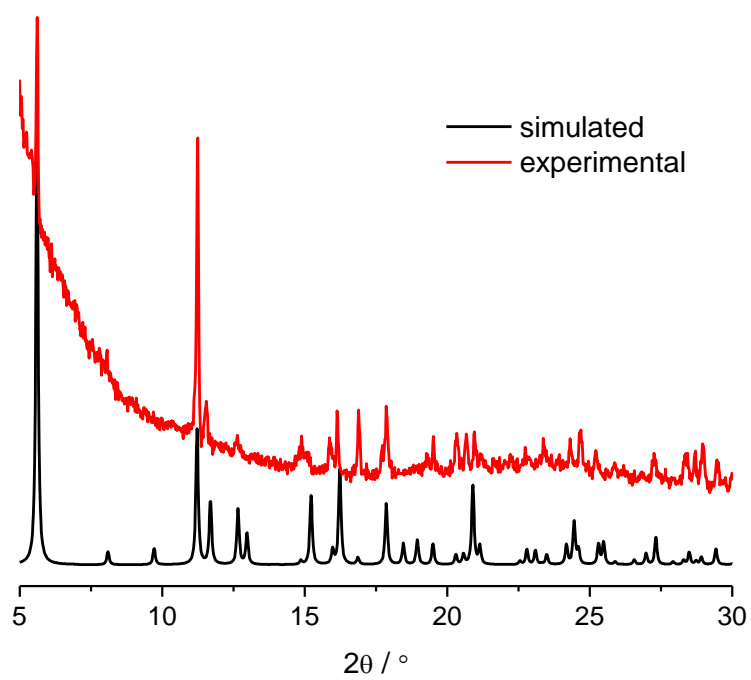
Fig. S11. The PXRD profiles of compound **2**.